

Effective slip boundary conditions for arbitrary 1D surfaces

Evgeny S. Asmolov^{1,2,3} † and Olga I. Vinogradova^{1,4,5}

¹A.N. Frumkin Institute of Physical Chemistry and Electrochemistry, Russian Academy of Sciences, 31 Leninsky Prospect, 119991 Moscow, Russia

²Central Aero-Hydrodynamic Institute, 140180 Zhukovsky, Moscow region, Russia

³Institute of Mechanics, M. V. Lomonosov Moscow State University, 119991 Moscow, Russia

⁴Department of Physics, M. V. Lomonosov Moscow State University, 119991 Moscow, Russia

⁵DWI, RWTH Aachen, Forckenbeckstr. 50, 52056 Aachen, Germany

(Received 6 September 2018)

In many applications it is advantageous to construct effective slip boundary conditions, which could fully characterize flow over patterned surfaces. Here we focus on laminar shear flows over smooth anisotropic surfaces with arbitrary scalar slip $b(y)$, varying in only one direction. We derive general expressions for eigenvalues of the effective slip-length tensor, and show that the transverse component is equal to a half of the longitudinal one with twice larger local slip, $2b(y)$. A remarkable corollary of this relation is that the flow along any direction of the 1D surface can be easily determined, once the longitudinal component of the effective slip tensor is found from the known spatially nonuniform scalar slip.

1. Introduction

With recent advances in microfluidics (Stone *et al.* 2004), renewed interest has emerged in quantifying the effects of surface chemical heterogeneities with a different local scalar slip on fluid motion. In this situation it is advantageous to construct the effective slip boundary condition, which is applied at the imaginary smooth homogeneous, but generally anisotropic surface, and mimics the actual one along the true heterogeneously slipping surface (Vinogradova & Belyaev 2011; Kamrin *et al.* 2010). Such an effective condition fully characterizes the flow at the real surface (on the scale larger than the pattern characteristic length) and can be used to solve complex hydrodynamic problems without tedious calculations.

For an anisotropic texture, the effective boundary condition generally depends on the direction of the flow and is a tensor, $\mathbf{b}_{\text{eff}} \equiv \{b_{ij}^{\text{eff}}\}$ represented by a symmetric, positive definite 2×2 matrix (Bazant & Vinogradova 2008)

$$\mathbf{b}_{\text{eff}} = \mathbf{S}_\theta \begin{pmatrix} b_{\text{eff}}^\parallel & 0 \\ 0 & b_{\text{eff}}^\perp \end{pmatrix} \mathbf{S}_{-\theta}, \quad (1.1)$$

diagonalized by a rotation

$$\mathbf{S}_\theta = \begin{pmatrix} \cos \theta & \sin \theta \\ -\sin \theta & \cos \theta \end{pmatrix}.$$

† Author to whom correspondence should be addressed; email: aes50@yandex.ru

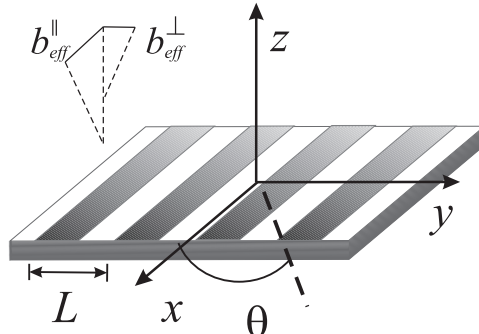


FIGURE 1. Schematic representation of periodic textures with scalar slip boundary conditions, varying in direction y . The patterns of slip boundary conditions are depicted as alternating stripes with piecewise constant slip lengths, but our discussion is more general and applies to any 1D distribution of a local slip (e.g., sinusoidal, trapezoidal, and more).

Therefore, Eq.(1.1) allows us to calculate an effective slip in any direction given by an angle θ . In other words, the general problem reduces to computing the two eigenvalues, $b_{\text{eff}}^{\parallel}$ ($\theta = 0$) and b_{eff}^{\perp} ($\theta = \pi/2$), which attain the maximal and minimal directional slip lengths, respectively. This tensorial slip approach, based on a consideration of a ‘macroscale’ fluid motion instead of solving hydrodynamic equations at the scale of the individual pattern, was supported by statistical diffusion arguments (Bazant & Vinogradova 2008), and was recently justified for the case of Stokes flow over a broad class of periodic surfaces (Kamrin *et al.* 2010).

The concept of an effective tensorial slip has recently been proven by simulations (Priezjev 2011; Schmieschek *et al.* 2012), and was already used to obtain simple solutions of several complex problems. It may be useful in many situations, such as drainage of thin films (Belyaev & Vinogradova 2010b; Asmolov *et al.* 2011), mixing in superhydrophobic channels (Vinogradova & Belyaev 2011), and electrokinetics of patterned surfaces (Bahga *et al.* 2010; Belyaev & Vinogradova 2011). However, to the best of our knowledge all these analytical solutions were obtained for a flow on alternating slip and no-slip stripes, and the quantitative understanding of effective slippage past other types of anisotropic surfaces is still challenging.

In this paper, we study the Stokes flow past flat surfaces, where the local (scalar) slip length b varies only in one direction. Our focus is on the limit of a thick (compared to texture period) channel or a single interface, so that effective slip is a characteristics of a heterogeneous interface solely and does not depend on the channel thickness. We derive a simple universal relationship between eigenvalues of the slip-length tensor. This allows one to avoid tedious calculations of flows in a transverse configuration, by reducing the problem to an analysis of longitudinal flows, which is much easier to evaluate. Our results open a possibility to solve a broad class of hydrodynamic problems for 1D textured surfaces.

2. Theory

2.1. General consideration

We consider a creeping flow along a plane anisotropic wall, and a Cartesian coordinate system (x, y, z) (Fig. 1). The origin of coordinates is placed at the flat interface, characterized by a slip length $b(y)$, spatially varying in one direction, and the texture varies over

a period L . Our analysis is based on the limit of a thick channel or a single interface, so that the velocity profile sufficiently far above the surface, at a height may be considered as a linear shear flow. Note that our results do not apply to a thin or an arbitrary channel situation, where the effective slip scales with the channel width (Feuillebois *et al.* 2009; Schmieschek *et al.* 2012).

Dimensionless variables are defined by using L as a reference length scale, the shear rate sufficiently far above the surface, G , and the fluid kinematic viscosity, ν . We seek the solution for the velocity profile in the form

$$\mathbf{v} = \mathbf{U} + \mathbf{u}_1,$$

where $\mathbf{U} = z\mathbf{e}_l$, $l = x, y$, is the undisturbed linear shear flow, \mathbf{e}_l are the unit vectors. The perturbation of the flow, $\mathbf{u}_1 = (u, v, w)$, which is caused by the presence of the texture and decays far from the surface at small Reynolds number $Re = GL^2/\nu$ satisfies dimensionless Stokes equations,

$$\begin{aligned} \nabla \cdot \mathbf{u}_1 &= 0, \\ \nabla p - \Delta \mathbf{u}_1 &= 0, \end{aligned} \quad (2.1)$$

where p is pressure. The boundary conditions at the wall and at infinity are defined in the usual way

$$z = 0: \quad \mathbf{u}_{1\tau} - \beta(y) \frac{\partial \mathbf{u}_{1\tau}}{\partial z} = \beta(y) \mathbf{e}_l, \quad (2.2)$$

$$w = 0, \quad (2.3)$$

$$z \rightarrow \infty: \quad \frac{\partial \mathbf{u}_1}{\partial z} = \mathbf{0}, \quad (2.4)$$

where $\mathbf{u}_{1\tau} = (u, v, 0)$ is the velocity along the wall and $\beta = b/L$ is the normalized slip length.

A local slip length can be expanded in a Fourier series

$$\beta(y) = \sum_{n=-\infty}^{\infty} b^*(n) \exp(ik_n y),$$

$$k_n = 2\pi n.$$

Similarly, the solution to (2.1) for \mathbf{u}_1 and p has the form

$$\mathbf{u}_1 = \sum_{n=-\infty}^{\infty} \mathbf{u}^*(n, z) \exp(ik_n y), \quad p = \sum_{n=-\infty}^{\infty} p^*(n, z) \exp(ik_n y), \quad (2.5)$$

and the Stokes equations can then be rewritten as

$$\nabla^* \cdot \mathbf{u}^* = 0, \quad (2.6)$$

$$\nabla^* p^* - \Delta^* \mathbf{u}^* = \mathbf{0}, \quad (2.7)$$

$$\nabla^* = \left(0, ik_n, \frac{d}{dz} \right), \quad \Delta^* = \frac{d^2}{dz^2} - k_n^2.$$

We have therefore reduced the problem to the system of ordinary differential equations (ODE), which can be now solved analytically. Similar strategy has been used before to address different hydrodynamic problems (Asmolov 2008; Kamrin *et al.* 2010).

The zero mode solution represents a constant, $\mathbf{u}^*(0, z) = (c_x(0), c_y(0), 0)$. The eigen-

values of the effective slip-length tensor can be obtained as the components of $\mathbf{u}^*(0, z)$:

$$b_{\text{eff}}^{\parallel} = Lc_x(0), \quad b_{\text{eff}}^{\perp} = Lc_y(0). \quad (2.8)$$

Below we analyze in more details two configurations of the shear flow, where the slip regions are distributed parallel ($\theta = 0$) and transverse ($\theta = \pi/2$) to the shear flow direction.

2.2. Longitudinal configuration

For longitudinal patterns, $\mathbf{U} = z\mathbf{e}_x$, so that the perturbation of the velocity has the only one component, $\mathbf{u}_1 = (u, 0, 0)$, and the system (2.6)-(2.7) reduces to a single ODE:

$$\Delta^* u^* = 0. \quad (2.9)$$

Its decaying at infinity solution for non-zero modes has the form

$$u^* = c_x(n) \exp(-|k_n|z). \quad (2.10)$$

The boundary condition at the wall, (2.2), then determines constants $c_x(n)$. Indeed, from (2.5) and (2.10) we get

$$z = 0: \quad u = \sum_{n=-\infty}^{\infty} c_x(n) \exp(ik_n y), \quad \frac{\partial u}{\partial z} = - \sum_{n=-\infty}^{\infty} |k_n| c_x(n) \exp(ik_n y),$$

so that (2.2) takes the form

$$c_x(n) + \sum_{m=-\infty}^{\infty} |k_m| c_x(m) b^*(n-m) = b^*(n), \quad (2.11)$$

where $b^*(n)$ is the Fourier coefficient of the slip length. Thus we reduce the longitudinal problem to the infinite linear system for $c_x(n)$, which can be found by truncating the system and by using standard routines for linear systems.

2.3. Transverse configuration

For transverse patterns, $\mathbf{U} = z\mathbf{e}_y$ and $\mathbf{u}_1 = (0, v, w)$, the solution is usually constructed using the vorticity $\omega = \nabla \times \mathbf{u}_1 = (0, 0, \omega_z)$, which significantly complicates the analysis as compared to a longitudinal case (Cottin-Bizonne *et al.* 2004; Priezjev *et al.* 2005; Belyaev & Vinogradova 2010a). However, simple analytical solutions can be obtained directly for the Fourier coefficients of velocities (Asmolov 2008; Kamrin *et al.* 2010). Indeed, equations (2.6)-(2.7) for transverse stripes can be written as

$$\begin{aligned} ik_n v^* + \frac{dw^*}{dz} &= 0, \\ ik_n p^* - \Delta^* v^* &= 0, \\ \frac{dp^*}{dz} - \Delta^* w^* &= 0. \end{aligned} \quad (2.12)$$

By excluding p^* and v^* , one can transform them to a single ODE for the z -component:

$$\Delta^{*2} w^* = 0, \quad (2.13)$$

$$z = 0; \quad z \rightarrow +\infty: \quad w^* = 0. \quad (2.14)$$

A general solution of the fourth-order ODE (2.13) decaying at infinity can be written as

$$w^* = (c_z + d_z z) \exp(-|k_n|z).$$

Condition (2.14) then determines the coefficient, $c_z = 0$. The velocity Fourier coefficient in y -direction can also be obtained from the first Eq. (2.12):

$$v^* = c_y \exp(-|k_n|z)(1 - |k_n|z), \quad (2.15)$$

with $c_y = id_z/k_n$, so that

$$w^* = -ik_n c_y z \exp(-|k_n|z). \quad (2.16)$$

Thus the solution for a given Fourier mode involves only one unknown constant $c_y(n)$, which can be found by applying boundary conditions (2.2). Using (2.5) and (2.15), we then get

$$z = 0 : \quad v = \sum_{n=-\infty}^{\infty} c_y(n) \exp(ik_n y), \quad \frac{\partial v}{\partial z} = -2 \sum_{n=-\infty}^{\infty} |k_n| c_y(n) \exp(ik_n y),$$

so that the slip boundary condition (2.2) can be rewritten as

$$c_y(n) + 2 \sum_{m=-\infty}^{\infty} |k_m| c_y(m) b^*(n-m) = b^*(n). \quad (2.17)$$

The system (2.17) is very similar to that for the longitudinal patterns, (2.11), and differs only by the prefactor of 2. This means that the solution for $c_y(n)$ can be expressed in terms of coefficients $c_{x2}(n)$ for the longitudinal flow with twice larger local slip, $b_2(y) = 2b(y)$. Since $b_2^*(n) = 2b^*(n)$, we obtain from (2.11):

$$c_{x2}(n) + 2 \sum_{m=-\infty}^{\infty} |k_m| c_{x2}(m) b^*(n-m) = 2b^*(n). \quad (2.18)$$

The left-hand sides of the linear systems (2.17) and (2.18) are identical, but the right-hand sides differ by the factor of 2. In what follows,

$$c_y(n) = \frac{c_{x2}(n)}{2}. \quad (2.19)$$

Whence by using (2.8) we get

$$b_{\text{eff}}^{\perp} [b(y)/L] = \frac{b_{\text{eff}}^{\parallel} [2b(y)/L]}{2}. \quad (2.20)$$

Thus, the longitudinal and transverse effective slip lengths are affine, being related by a simple formula.

3. Discussion

In this section we compare Eq.(2.20) with the results obtained earlier for some particular periodic textures spatially varying in one direction y along the surface. We also make use of Eq.(2.19) to prove a similarity of velocity profiles in eigendirections, again by giving some supporting examples from prior work. Finally, we show that our results are valid for arbitrary, not necessarily periodic, 1D textures (varying on a characteristic scale L).

3.1. Effective slip length

During the last few decades several theoretical papers have been concerned with the flow past alternating (parallel or transverse) stripes characterized by piecewise constant, slip

lengths, b^+ and b^- with area fractions ϕ^+ and $\phi^- = 1 - \phi^+$, correspondingly. Without loss of generality we consider below that $0 \leq b^- \leq b^+ < \infty$. A large fraction of these papers deals with an ideal case of stripes with $b^+ \gg L$ (perfect slip) and $b^- = 0$ (no-slip). The formula describing the effective slip in longitudinal direction for such a texture was proposed by Philip (1972):

$$b_{\text{ideal}}^{\parallel} = \frac{L}{\pi} \ln \left[\sec \left(\frac{\pi\phi^+}{2} \right) \right] \quad (3.1)$$

Later Lauga & Stone (2003) derived an expression for the transverse configuration:

$$b_{\text{ideal}}^{\perp} = \frac{L}{2\pi} \ln \left[\sec \left(\frac{\pi\phi^+}{2} \right) \right], \quad (3.2)$$

which suggested that transverse and longitudinal components of the slip-length tensor are related as

$$b_{\text{ideal}}^{\perp} = \frac{b_{\text{ideal}}^{\parallel}}{2}. \quad (3.3)$$

This relationship is consistent with predictions of Eq.(2.20). Note that Eq.(3.3) should be valid not only for regular textures, shown in Fig. 1, but also for periodic textures including several stripes of differing widths, e.g., for hierarchical fractal surfaces (Cottin-Bizonne *et al.* 2012).

A few authors have discussed a situation of $b^- = 0$ and finite b^+ . Numerical data obtained by Cottin-Bizonne *et al.* (2004) seem to satisfy Eq.(2.20), and their $b_{\text{eff}}^{\parallel}$, b_{eff}^{\perp} asymptotically tend to the limiting values, $b_{\text{ideal}}^{\parallel}$ and b_{ideal}^{\perp} , when b^+/L becomes large. Belyaev & Vinogradova (2010a) derived analytical expressions for this case

$$b_{\text{eff}}^{\parallel} \simeq \frac{L}{\pi} \frac{\ln \left[\sec \left(\frac{\pi\phi^+}{2} \right) \right]}{1 + \frac{L}{\pi b^+} \ln \left[\sec \left(\frac{\pi\phi^+}{2} \right) + \tan \left(\frac{\pi\phi^+}{2} \right) \right]},$$

$$b_{\text{eff}}^{\perp} \simeq \frac{L}{2\pi} \frac{\ln \left[\sec \left(\frac{\pi\phi^+}{2} \right) \right]}{1 + \frac{L}{2\pi b^+} \ln \left[\sec \left(\frac{\pi\phi^+}{2} \right) + \tan \left(\frac{\pi\phi^+}{2} \right) \right]},$$

which are again in agreement with predictions of Eq.(2.20).

Ng & Wang (2009) addressed the problem of effective slip lengths for stripes with $b^+ \gg L$ and partial b^- , and obtained

$$b_{\text{eff}}^{\parallel} \simeq b_{\text{ideal}}^{\parallel} + \frac{b^-}{\phi^-}, \quad b_{\text{eff}}^{\perp} \simeq b_{\text{ideal}}^{\perp} + \frac{b^-}{\phi^-}.$$

It can be seen, that this result also satisfies Eq.(2.20).

For a weakly slipping anisotropic texture, $b(x, y) \ll L$, the area-averaged isotropic slip length has been predicted (Belyaev & Vinogradova 2010a). This means that the slip length tensor becomes isotropic and for all in-plane directions, the flow aligns with the applied shear stress. Similar conclusion has been made by Kamrin *et al.* (2010). They proposed asymptotic solutions for \mathbf{b}_{eff} for a weakly slipping interface, $\varepsilon = \max |b^*(n)| \ll 1$. The two-term expansions of the effective slip lengths in ε can be obtained for an arbitrary local slip :

$$b_{\text{eff}}^{\parallel}/L = b^*(0) - \sum_{n=-\infty}^{\infty} |k_n| |b^*(n)|^2, \quad b_{\text{eff}}^{\perp}/L = b^*(0) - 2 \sum_{n=-\infty}^{\infty} |k_n| |b^*(n)|^2. \quad (3.4)$$

Since $b_2^*(n) = 2b^*(n)$, Eq.(3.4) is also consistent with the relation (2.20).

These examples fully support our predictions, but of course Eq.(2.20) is universal and should hold for any 1D surface.

Moreover, Eq.(2.20) still holds when the flow is unsteady. Ng & Wang (2011) have considered pressure-driven oscillatory flow in a channel with walls patterned by stripes of $b^+ \gg L$ and $b^- = 0$. For a thick channel they found that both real and imaginary parts of the effective slip lengths roughly satisfy Eq.(3.3). The reason is that Eqs.(2.10), (2.11) and (2.15-2.17) remain valid in this case if one replaces $|k_n|$ by $\sqrt{k_n^2 + i\omega}$.

3.2. Flow field

We remark and stress that Eq.(2.19) allows one to express the entire flow field for the transverse configuration of patterns in terms of the longitudinal flow field, $u_2(y, z) = u[y, z, 2b(y)]$. Indeed, by applying the inverse Fourier transform of (2.15) and (2.16), one can easily derive by using (2.10), (2.12) and (2.19):

$$v = \frac{1}{2} \left(u_2 + z \frac{\partial u_2}{\partial z} \right), \quad w = -\frac{z}{2} \frac{\partial u_2}{\partial y}, \quad (3.5)$$

$$p = -\frac{\partial u_2}{\partial y}. \quad (3.6)$$

Whence we conclude that at the wall

$$z = 0: \quad v = \frac{1}{2}u_2, \quad \frac{\partial v}{\partial z} = \frac{\partial u_2}{\partial z}. \quad (3.7)$$

Several important conclusions follow from (3.5), (3.6) for alternating perfect slip ($b^+ \gg L$) and no-slip stripes ($b^- = 0$). In this case $u_2 = u$, and hence, at the wall the velocity along this 1D texture is always twice that of perpendicular to it, $u = 2v$. The same relation between velocities in eigendirections has been found by Teo & Khoo (2009) and Ng *et al.* (2010) for the pressure-driven flow in a wide grooved superhydrophobic channel. Analytical solutions have been obtained for the longitudinal velocity u and its gradient $\partial u/\partial y$ at the wall for the shear flow (Sbragaglia & Prosperetti 2007). Eq.(3.6) enables us to obtain the pressure for the transverse flow over the perfect-slip region, $|y| \leq \phi^+/2$:

$$z = 0: \quad p = -\frac{\partial u}{\partial y} = \frac{\sin(\pi y)}{\sqrt{\cos^2(\pi y) - \cos^2(\pi\phi^+/2)}}. \quad (3.8)$$

The pressure over the no-slip regions, $\phi^+/2 \geq |y| \geq 1/2$, where $\partial u/\partial y = 0$, is zero. The distribution (3.8) calculated for $\phi^+ = 0.7$ is shown in Fig. 2. It grows infinitely near the jump in $b(y)$ (from $b^+ \gg L$ to $b^- = 0$) at $y = \pm\phi^+/2$:

$$p \simeq \pm \sin(\pi\phi^+/2) [\pi \sin(\pi\phi^+) s]^{-1/2} \quad \text{as } s = (\phi^+/2 - |y|) \rightarrow +0. \quad (3.9)$$

Note that a solution for a velocity in an arbitrary direction of the undisturbed flow, $\mathbf{U} = z(\mathbf{e}_x \cos \theta + \mathbf{e}_y \sin \theta)$, represents a superposition of solutions in eigendirections:

$$\mathbf{u}_1 = u\mathbf{e}_x \cos \theta + (v\mathbf{e}_y + w\mathbf{e}_z) \sin \theta.$$

Therefore, the knowledge about the longitudinal velocity at the wall allows us to calculate the flow field in any direction given by an angle θ .

3.3. Surfaces with an arbitrary 1D texture

Up to this point, our focus has been on periodic 1D surface. Now, we can remove all periodicity requirements we used to derive Eq.(2.19) by applying the Fourier analysis.

[tbp]

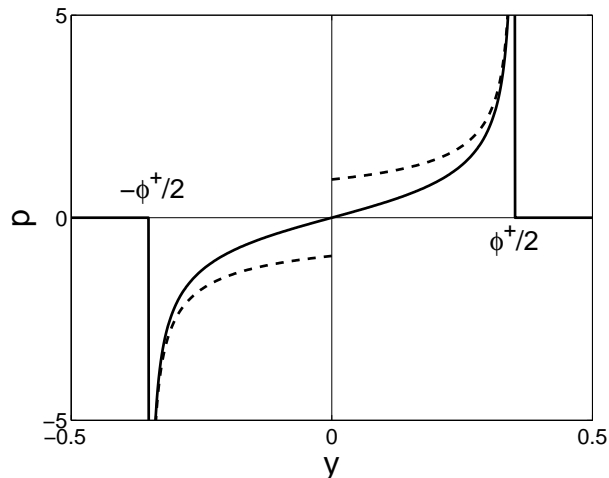


FIGURE 2. Pressure distribution in the transverse flow over alternating perfect-slip, $|y| \leq \phi^+/2$, and no-slip, $\phi^+/2 \geq |y| \geq 1/2$, stripes. Solid and dashed lines are Eqs. (3.8) and (3.9), respectively.

Indeed, if u_2 is the solution of the longitudinal problem with a non-periodic slip length $2L\beta(y)$, satisfying

$$\Delta u_2 = 0,$$

$$z = 0: \quad u_2 - 2\beta(y) \frac{\partial u_2}{\partial z} = 2\beta(y),$$

then one can verify directly that transverse solutions, Eqs.(3.5), (3.6), taking into account (3.7), satisfy the Stokes equation (2.1) and boundary conditions (2.2), (2.3). Thus, our results are valid for any arbitrary patterned, not necessarily periodic, 1D surfaces.

Acknowledgement

This research was supported by the Russian Academy of Sciences through its Priority Programme ‘Assembly and Investigation of Macromolecular Structures of New Generations’

REFERENCES

- ASMOLOV, E. S. 2008 Shear-induced self-diffusion in a wall-bounded dilute suspension. *Phys. Rev. E* **77** (6), 66312.
- ASMOLOV, E. S., BELYAEV, A. V. & VINOGRADOVA, O. I. 2011 Drag force on a sphere moving towards an anisotropic super-hydrophobic plane. *Phys. Rev. E* **84**, 026330.
- BAHGA, S. S., VINOGRADOVA, O. I. & BAZANT, M. Z. 2010 Anisotropic electro-osmotic flow over super-hydrophobic surfaces. *J. Fluid Mech.* **644**, 245–255.
- BAZANT, M. Z. & VINOGRADOVA, O. I. 2008 Tensorial hydrodynamic slip. *J. Fluid Mech.* **613**, 125–134.
- BELYAEV, A. V. & VINOGRADOVA, O. I. 2010a Effective slip in pressure-driven flow past super-hydrophobic stripes. *J. Fluid Mech.* **652**, 489–499.
- BELYAEV, A. V. & VINOGRADOVA, O. I. 2010b Hydrodynamic interaction with super-hydrophobic surfaces. *Soft Matter* **6**, 4563–4570.

- BELYAEV, A. V. & VINOGRADOVA, O. I. 2011 Electro-osmosis on anisotropic super-hydrophobic surfaces. *Phys. Rev. Lett.* **107**, 098301.
- COTTIN-BIZONNE, C., BARENTIN, C. & BOCQUET, L. 2012 Scaling laws for slippage on super-hydrophobic fractal surfaces. *Phys. Fluids* **24**, 012001.
- COTTIN-BIZONNE, C., BARENTIN, C., CHARLAIX, E., BOCQUET, L. & BARRAT, J. L. 2004 Dynamics of simple liquids at heterogeneous surfaces: Molecular-dynamics simulations and hydrodynamic description. *Eur. Phys. J. E* **15** (4), 427–438.
- FEUILLEBOIS, F., BAZANT, M. Z. & VINOGRADOVA, O. I. 2009 Effective slip over superhydrophobic surfaces in thin channels. *Phys. Rev. Lett.* **102**, 026001.
- KAMRIN, K., BAZANT, M. Z. & STONE, H. A. 2010 Effective slip boundary conditions for arbitrary periodic surfaces: the surface mobility tensor. *J. Fluid Mech.* **658**, 409–437.
- LAUGA, E. & STONE, H. A. 2003 Effective slip in pressure-driven Stokes flow. *J. Fluid Mech.* **489**, 55–77.
- NG, C.O., CHU, H.C.W. & WANG, C.Y. 2010 On the effects of liquid-gas interfacial shear on slip flow through a parallel-plate channel with superhydrophobic grooved walls. *Phys. Fluids* **22** (10), 102002.
- NG, C.O. & WANG, C.Y. 2009 Stokes shear flow over a grating: Implications for superhydrophobic slip. *Phys. Fluids* **21** (1), 013602.
- NG, C.O. & WANG, C.Y. 2011 Oscillatory flow through a channel with stick-slip walls: Complex Navier’s slip length. *J. Fluids Eng.* **133**, 014502.
- PHILIP, J. R. 1972 Flows satisfying mixed no-slip and no-shear conditions. *J. Appl. Math. Phys.* **23**, 353–372.
- PRIEZJEV, N. V. 2011 Molecular diffusion and slip boundary conditions at smooth surfaces with periodic and random nanoscale textures. *J. Chem. Phys.* **135**, 204704.
- PRIEZJEV, N. V., DARHUBER, A. A. & TROIAN, S. M. 2005 Slip behavior in liquid films on surfaces of patterned wettability. *Phys. Rev. E* **71**, 041608.
- SBRAGAGLIA, M. & PROSPERETTI, A. 2007 A note on the effective slip properties for microchannel flows with ultrahydrophobic surfaces. *Phys. Fluids* **19**, 043603.
- SCHMIESCHEK, S., BELYAEV, A. V., HARTING, J. & VINOGRADOVA, O. I. 2012 Tensorial slip of super-hydrophobic channels. *Phys. Rev. E* **85**, 016324.
- STONE, H. A., STROOCK, A. D. & AJDARI, A. 2004 Engineering flows in small devices. *Annual Review of Fluid Mechanics* **36**, 381–411.
- TEO, C. & KHOO, B. 2009 Analysis of Stokes flow in microchannels with superhydrophobic surfaces containing a periodic array of micro-grooves. *Microfluid Nanofluid* **7**, 353.
- VINOGRADOVA, O. I. & BELYAEV, A. V. 2011 Wetting, roughness and flow boundary conditions. *J. Phys.: Condens. Matter* **23**, 184104.